Optical Materials 58 (2016) 14–17

Contents lists available at ScienceDirect

Optical Materials

journal homepage: www.elsevier.com/locate/optmat

Crystal growth and luminescence properties of $Yb_2Si_2O_7$ infra-red emission scintillator

Takahiko Horiai [a, *], Shunsuke Kurosawa [b, **], Rikito Murakami [a], Jan Pejchal [c], Akihiro Yamaji [a], Yasuhiro Shoji [a, d], Valery I. Chani [a], Yuji Ohashi [a], Kei Kamada [b, d], Yuui Yokota [b], Akira Yoshikawa [a, b, d]

[a] Institute for Materials Research, Tohoku University, 2-1-1 Katahira, Aoba-ku, Sendai, Miyagi, 980-8577, Japan
[b] New Industry Creation Hatchery Center (NICHe), Tohoku University, 6-6-10 Aoba, Aramaki, Aoba-ku, Sendai, Miyagi, 980-8579, Japan
[c] Institute of Physics CAS, Cukrovamicka 10, Prague 162 00, Czech Republic
[d] C&A Corporation, 6-6-40 Aoba, Aramaki, Aoba-ku, Sendai, Miyagi 980-8579, Japan

ARTICLE INFO

Article history:
Received 12 February 2016
Received in revised form
15 April 2016
Accepted 15 April 2016

Keywords:
Scintillator
Pyrosilicate
Charge transfer
Infra-red
Single crystal

ABSTRACT

$(Ce_xYb_{1-x})_2Si_2O_7$ (x = 0.00, 0.01) single crystals were grown by the micro-pulling-down method to test the possibility of its application as infra-red scintillator for medical imaging. Powder X-ray diffraction analysis indicated that the crystals were single-phase materials. The radioluminescence spectra of the crystals demonstrated presence of two near infra-red emission peaks (at 1010 and 1030 nm). The emission peaks at 420 and 580 nm ascribed to defects were also observed in the crystals. The human body has maximum transmission in wavelength range from 650 to 1200 nm. Therefore, $Yb_2Si_2O_7$ is expected to be used as efficient infra-red scintillator for medical applications.

1. Introduction

Radiation therapy is one of the widely-used tumor treatments that uses high-energy particles or X/gamma rays to destroy cancer cells [1]. However, medical accidents such as over- or under-exposure occur occasionally when such treatment is applied [2]. Therefore, the real-time monitoring of radiation dose is required to increase the security of radiation treatment. One of the ideas used to control the radiation dose is based on application of a probe, which consists of optical fiber with small volume scintillator [3]; X-rays generate considerable noise in the fiber.

Recently, implantable real time dose monitoring system using infra-red scintillators has been also proposed (Fig. 1) [4–7]. In such a system, the light output from the infra-red scintillator can be proportional to the X-ray dose. Thus, the resulting scintillation photons can propagate through the human tissue and can be read-out with photon detectors such as Charge-Coupled Device (CCD) camera or Complementary metal–oxide–semiconductor (CMOS) camera positioned outside of the patient's body.

In the previous studies, scintillation properties of Yb-doped $Gd_3Al_2Ga_3O_{12}$ (Yb:GAGG), Cr-doped $Gd_3Ga_5O_{12}$ (Cr:GGG) and Nd-doped Lu_2O_3 as near-infra-red (NIR) scintillators were examined [4–7]. Regarding the application discussed here, the implantable scintillator must have small size of ~3 mm in diameter. Additionally, the scintillating material should have a high effective atomic number to establish acceptable X-ray detection efficiency [8]. However, Yb:GAGG and Cr:GGG have low effective atomic numbers of 51 and 50, respectively. On the other hand, Nd:Lu_2O_3 has relatively high effective atomic number of 67. However, Lu has large intrinsic gamma-rays background due to ^{176}Lu isotope, which is not suitable for the patient.

To develop novel scintillator with NIR emission and comparatively high effective atomic number, we focused on $Yb_2Si_2O_7$ (YbPS), because (i) Yb^{3+} 4f–4f emission wavelength is expected to be in the NIR region [4], (ii) YbPS has effective atomic number ($Z_{eff}(Yb_2Si_2O_7) = 60$) which is greater than that of GAGG and GGG, (iii) YbPS melts congruently and can be produced in the single

* Corresponding author.
** Corresponding author.
E-mail addresses: horiai@imr.tohoku.ac.jp (T. Horiai), kurosawa@imr.tohoku.ac.jp (S. Kurosawa).

http://dx.doi.org/10.1016/j.optmat.2016.04.032
0925-3467/

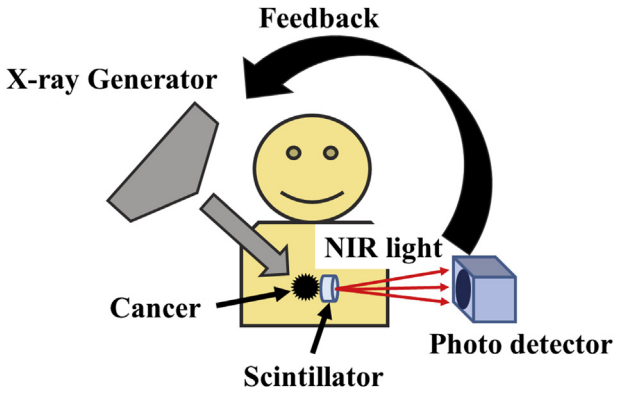

Fig. 1. Schematic diagram of the implantable real-time dosimeter system.

crystal form by the melt growth methods [9,10], and (iv) Yb, Si and O have negligible natural abundance of radio-active isotopes and are good constituents for the material without intrinsic background.

According to our knowledge, the luminescent properties of YbPS were not examined in the past. Moreover, $Yb_2Si_2O_7$ single crystal growth was not reported except fabrication of nanocrystals and polycrystalline materials [11]. Thus, the purpose of this research was to produce relatively large mm-scale $Yb_2Si_2O_7$ single crystals and to study their optical and scintillation properties. The crystal growth was performed from the melt using the micro-pulling-down (μ-PD) method [12]. This technique is often considered as fast crystal growth method that allows production of mm-scale crystals within one day.

Some Yb-containing materials such as Yb-doped $Y_3Al_5O_{12}$ (Yb:YAG) have been reported to have charge transfer (CT) emission around 330 and 490 nm [13]. Since it is the first communication on optical properties of the $Yb_2Si_2O_7$ crystal, we also evaluated the CT emission in the interval from ~7.5 K to room temperature (RT). Additionally, Ce and Yb co-doped YAG demonstrated blue-to-NIR conversion that is established via the single-step mechanism of energy transfer through a Ce^{4+}-Yb^{2+} charge transfer state (CTS) [14]. Therefore, the optical properties of Ce-doped YbPS crystals grown by the μ-PD method are also discussed in the current report. Moreover, the comparison of the light outputs of undoped and Ce-doped $Yb_2Si_2O_7$ crystals excited by X-ray was also performed.

2. Materials and methods

Undoped and 1%Ce-doepd $Yb_2Si_2O_7$ single crystals were grown by the μ-PD method with a pulling rate of 0.05 mm/min in N_2 gas atmosphere [12]. The starting mixtures were prepared from Yb_2O_3, SiO_2 (and CeO_2) powders with purities of 99.99%. The crystals were grown using an Ir crucible and thin Ir rod as a seed. The phase identification of the as produced materials was performed by powder X-ray diffraction (XRD) analysis using a RINT 2000 (RIGAKU) apparatus. The crystals were cut and polished to produce specimens suitable for investigation of optical and scintillation properties.

Transmittance spectra were recorded with a spectrometer (V-670ST, JASCO) at RT. Photoluminescence (PL) emission spectra from visible to NIR were measured with an absolute PL quantum yield measurement system consisting of a Xe lamp (150 W) as an excitation lamp and two photonic-multi-channel analyzers with wavelength dynamic rages of 200–950 nm and 350–1100 nm for C10027-01 PMA-12 and C10027-02 PMA-12 (Hamamatsu), respectively [15].

Since detection of CT emission was expected, temperature dependences of PL emission spectra were evaluated within 7.5–300 K for both undoped and Ce-doped samples. The samples were irradiated with excitation photons from Beam line 3B of the Ultraviolet Synchrotron Orbital Radiation Facility III (UVSOR-III) located at the Institute for Molecular Science in Okazaki, Japan, and the samples were cooled down to 7.5 K with liquid helium. The emission spectra were examined with a spectrometer (spectoropro-300i, Acton research).

The radioluminescence spectra were measured with two spectrometers with a detection wavelength dynamic range of 190–800 nm and 800–1090 nm (DU420-OE and DU920-BEX-DD, respectively, ANDOR), when the specimens were excited by X-ray from the same X-ray generator used in XRD analysis (RINT 2000, RIGAKU) with an accelerating voltage of 40 kV and a beam current of 40 mA.

3. Results and discussions

The obtained bulk crystals of undoped YbPS and Ce:YbPS are compared in Fig. 2. Fig. 3 displays the results of powder XRD analysis of the crystals, which were consistent with previous available data for YbPS (JCPDS No. 25-1345). The crystalline structure of YbPS was monoclinic $C2/m$ and $a = 6.7991$, $b = 8.8734$, $c = 4.7084$ and $\beta = 101.969$ that is also consistent with previous data [16].

Fig. 4 shows transmission spectra for $(Ce_x\ Yb_{1-x})_2Si_2O_7$ ($x = 0.00$, 0.01) single crystalline specimens with thicknesses of 1 mm. The absorption peaks at 910 and 970 nm were ascribed to the absorption from the Yb^{3+} 4f–4f transition for both samples. Additionally to these peaks, strong absorption was observed at 300 and 350 nm for the Ce-doped $Yb_2Si_2O_7$ crystal due to the Ce^{3+} 4f–5d transitions. Both undoped and Ce-doped YbPS samples had absorption edges below 230 nm, and these absorptions originated from Yb^{3+}-O^{2-} charge transfer band or the absorption band of the YbPS host. Since the Ce-doped sample had no remarkable emission peaks originating from Yb^{3+} f–f transition in the NIR region when excited by ~300 or 350 nm photons (Ce^{3+} 4f–5d transition), the energy transfer from Ce to Yb was found to be inefficient in YbPS.

Additionally, $(Ce_{0.01}, Yb_{0.05}, Lu_{0.94})_2Si_2O_7$ sintered compact with much lower Yb concentration was prepared, and NIR emission peaks originating from Yb^{3+} f–f transition were observed under excitation around 350 nm (Fig. 5). This NIR emission would be due to energy transfer via a Ce^{4+}-Yb^{2+} charge transfer state [14]. Thus, the concentration quenching phenomenon occurring at high Yb

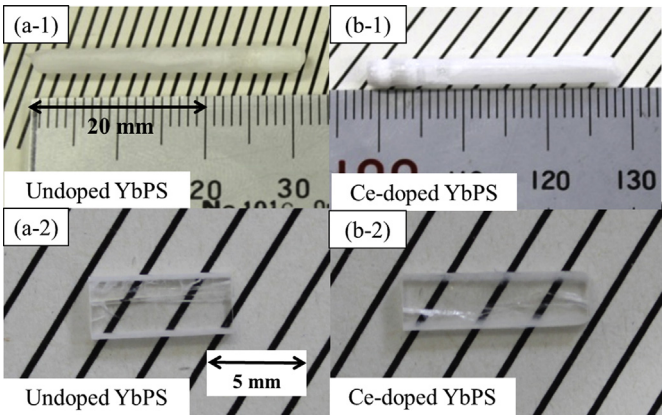

Fig. 2. Views of the as-grown $(Ce_x, Yb_{1-x})_2Si_2O_7$ ($x = 0.00$, 0.01) crystals prepared by the micro-pulling down method (a-1) and (b-1), and corresponding polished specimens (a-2) and (b-2) used for characterizations.

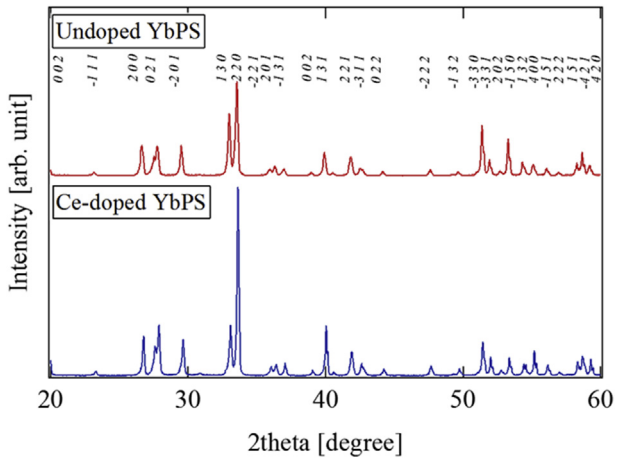

Fig. 3. Powder X-ray diffraction data for the $(Ce_x, Yb_{1-x})_2Si_2O_7$ (x = 0.00, 0.01) crystals (X-ray Source Target: Cu).

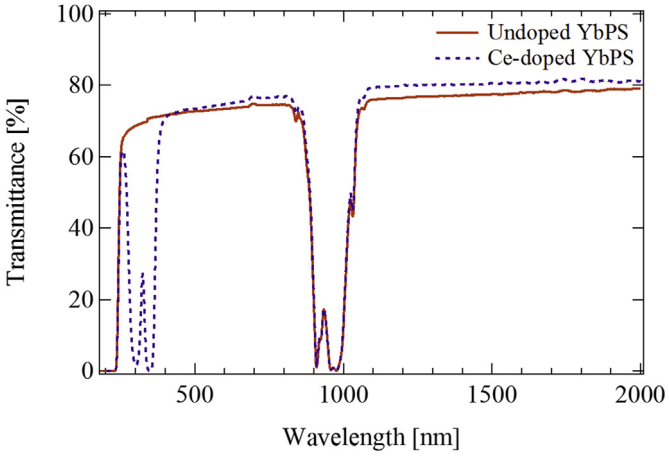

Fig. 4. Transmittance spectra of $(Ce_x, Yb_{1-x})_2Si_2O_7$ (x = 0.00, 0.01) measured between 190 and 2000 nm at room temperature.

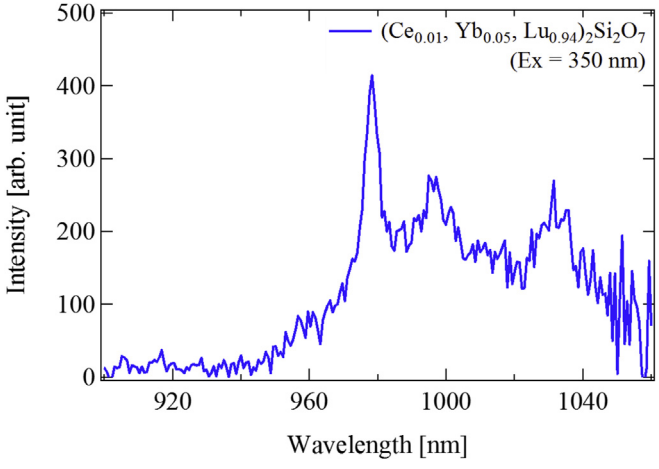

Fig. 5. Photoluminescence spectra of the $(Ce_{0.01}, Yb_{0.05}, Lu_{0.94})_2Si_2O_7$ sintered compact excited by 350 nm.

concentration can suppress the Yb emission.

Fig. 6 compares the temperature dependences of the PL

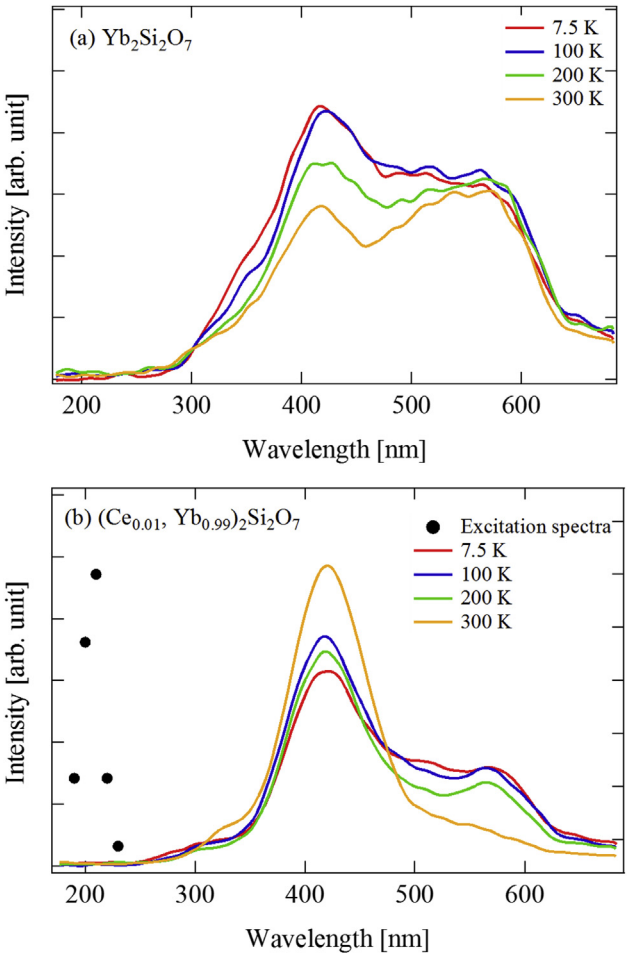

Fig. 6. Photoluminescence spectra of the $(Ce_x, Yb_{1-x})_2Si_2O_7$ (x = 0.00, 0.01) crystals measured at various temperatures.

emission spectra for the undoped (a) and Ce-doped (b) YbPS crystals under 210 nm excitation in the temperature range of 7.5–300 K. Since absorption edge was around 230 nm, the 210 nm photons were selected as an excitation source. Moreover, variations of the excitation wavelengths demonstrated that the strongest emission was observed at 210 nm excitation.

The undoped YbPS had emission peaks at around 420 and 580 nm. Although, the intensity of the 420 nm emission band decreased until 300 K, this peak still remained with detectable intensity at RT. On the other hand, intensity of the 580 nm band remained almost constant and independent on temperature. Thus, both the 420 nm and the 580 nm bands as being due to defects.

Oppositely, the intensity of the 420 nm emission band of the Ce-doped YbPS increased when temperature of the specimen became higher. It implied that the same defect as in the undoped YbPS is modified by Ce^{3+}. The 580 nm emission peak was also observed in the PL spectra of Ce-doped YbPS, while it was suppressed at RT.

The radioluminescence spectra for both crystals are illustrated in Fig. 7. The NIR emission peaks were ascribed to Yb^{3+} 4f–4f emission ($^2F_{5/2}$ to $^2F_{7/2}$). Although radioluminescence intensity of undoped YbPS was lower than that of the previously studied Yb-doped GAGG by an order of magnitude, YbPS has higher X-ray stopping power than Yb:GAGG by a factor of ~1.9 [7]. In addition, Gd is sometimes considered as toxic material that should be avoided [17]. Thus, YbPS is preferable for human body treatment in radiotherapy. As the infrared emission of YbPS was detected within the

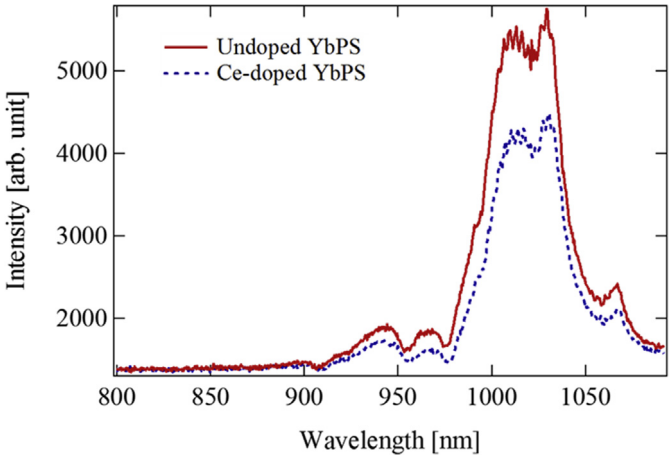

Fig. 7. Infra-red radioluminescence spectra of the $(Ce_x, Yb_{1-x})_2Si_2O_7$ (x = 0.00, 0.01) crystals.

"human window," application of this material in the dose monitors used during medical radiotherapy is proposed.

4. Conclusions

Successful growth of the $(Ce_x, Yb_{1-x})_2Si_2O_7$ (x = 0.00, 0.01) single crystals from the melt was demonstrated for the first time. The crystals were produced by the micro-pulling-down method. The photoluminescence and radioluminescence spectra measurements indicated presence of several luminescence peaks such as Yb^{3+} 4f–4f and defect luminescence. The Yb^{3+} 4f–4f emissions were detected at 1010 and 1030 nm, when the crystals were excited with a Xe lamp and X-ray. The NIR emission originating from Yb^{3+} 4f–4f transition energies is expected to be suitable for application in real time dose monitoring systems.

Acknowledgements

This work was partially supported by (i) Japan Society for the Promotion of Science KAKENHI Grant Number 14462961, 15597934, 15619740 (by Grant-in-Aid for Young Scientists(B), etc., S. Kurosawa), (ii) Bilateral AS CR–JSPS Joint Research Project sported at Czech side by MEYS, KONTAKT LH14266 grant, (iii) Japan Science and Technology Agency, Development of Systems and Technology for Advanced Measurement and Analysis (SENTAN), (iv) JST, Adaptable & Seamless Technology Transfer Program through Target-driven R&D, (v) the Association for the Progress of New Chemical Technology, (vi) The Murata Science Foundation, (vii) Nippon Sheet Glass Foundation for Materials Science and Engineering, (viii) Tonen General Sekiyu Foundation, (ix) Yazaki Memorial Foundation for Science and Technology, (x) Tokin Science and Technology Promotion Foundation, (xi) Intelligent cosmos research institute, (xii) Frontier Research Institute for Interdisciplinary Sciences, Tohoku University, and (xiii) the UVSOR Facility of the Institute for Molecular Science. In addition, we would like to thank following persons for their support: Mr. Yoshihiro Nakamura of Institute of Multidisciplinary Research for Advanced Materials (IMRAM), Tohoku University and Mr. Hiroshi Uemura, Ms. Keiko Toguchi, Ms. Megumi Sasaki, Ms. Yuka Takeda and Ms. Kuniko Kawaguchi of IMR, Tohoku University.

References

[1] A. Zerbi, V. Fossati, D. Parolini, M. Carlucci, G. Balzano, G. Bordogna, C. Staudacher, V.D. Calro, Cancer 73 (1994) 2930.
[2] J.M. Cosset, Radiother. Oncol. 63 (2002) 1.
[3] H.G. Low, W. Bonatz, W. Binder, Radiat. Prot. Dosim. 34 (1990) 283.
[4] A. Suzuki, S. Kurosawa, S. Nagata, T. Yamamura, J. Pejchal, A. Yamaji, Y. Yokota, K. Shirasaki, Y. Homma, D. Aoki, T. Shikama, A. Yoshikawa, Opt. Mater. 36 (2014) 1484.
[5] A. Yamaji, V.V. Kochurikhin, S. Kurosawa, A. Suzuki, Y. Fujimoto, Y. Yokota, A. Yoshikawa, IEEE Trans. Nucl. Sci. 61 (2014) 320.
[6] S. Kurosawa, L. An, A. Yamaji, A. Suzuki, Y. Yokota, K. Shirasaki, T. Yamamura, A. Ito, T. Goto, G. Boulon, A. Yoshikawa, IEEE Trans. Nucl. Sci. 61 (2014) 316.
[7] A. Suzuki, S. Kurosawa, A. Yamaji, Y. Shoji, J. Pejchal, K. Kamada, Y. Yokota, A. Yoshikawa, Opt. Mater. 36 (2014) 1938.
[8] F.W. Spiers, Br J. Radiol. 19 (1946) 52.
[9] N.A. Toropov, I.A. Bondar, Bull. Acad. Sci. USSR Div. Chem. Sci. 10 (1961) 1278.
[10] The American Ceramic Society and the National Institute of Standards and Technology, 2016. Figure Numbers 2391; www.nist.gov/srd/nist31.cfm.
[11] A.J. Fernandez-Carrion, M.D. Alba, A. Escudero, A.I. Becerro, J. Solid State Chem. 184 (2011) 1882.
[12] A. Yoshikawa, M. Nikl, G. Boulon, T. Fukuda, Opt. Mater. 30 (2007) 6.
[13] L. van Pieterson, M. Heeroma, E. de Heer, A. Meijerink, J. Lumin. 91 (2000) 177.
[14] D.C. Yu, F.T. Rabouw, W.Q. Boon, T. Kieboom, S. Ye, Q.Y. Zhang, A. Meijerink, Phys. Rev. B 90 (2014) 165126.
[15] S. Kurosawa, Y. Yokota, Y. Yanagida, J. Pejchal, A. Yamaji, Y. Shoji, K. Kamada, A. Yoshikawa, J. Cryst. Growth 393 (2014) 163.
[16] A.N. Christensen, New Cryst. Struct. 209 (1994) 7.
[17] M.A. Perazella, R.A. Rodby, Semin. Dial. 20 (2007) 179.